Heliyon 10 (2024) e29939

Contents lists available at ScienceDirect

Heliyon

journal homepage: www.cell.com/heliyon

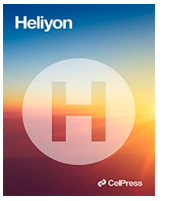

Research article

Exploring immune evasion of SARS-CoV-2 variants using a pseudotyped system

Haixiao Duan [a], Ershuai Zhang [a], Ge Ren [a], Yining Cheng [a], Binfeng Yang [b], Lirong Liu [b], Normand Jolicoeur [b], Han Hu [a], Yan Xu [b], Binlei Liu [a,b,*]

[a] National "111" Center for Cellular Regulation and Molecular Pharmaceutics, Key Laboratory of Fermentation Engineering (Ministry of Education), Hubei Provincial Cooperative Innovation Center of Industrial Fermentation, College of Bioengineering, Hubei University of Technology, Wuhan, China
[b] Wuhan Binhui Biopharmaceutical Co., Ltd., Wuhan, China

ARTICLE INFO

Keywords:
SARS-CoV-2
Pseudovirus
ACE2-mCherry-293T
Neutralization assay
Immune escape

ABSTRACT

In the United States, coronavirus disease 2019 (COVID-19) cases have consistently been linked to the prevailing variant XBB.1.5 of SARS-CoV-2 since late 2022. A system has been developed for producing and infecting cells with a pseudovirus (PsV) of SARS-CoV-2 to investigate the infection in a Biosafety Level 2 (BSL-2) laboratory. This system utilizes a lentiviral vector carrying ZsGreen1 and Firefly luciferase (Fluc) dual reporter genes, facilitating the analysis of experimental results. In addition, we have created a panel of PsV variants that depict both previous and presently circulating mutations found in circulating SARS-CoV-2 strains. A series of PsVs includes the prototype SARS-CoV-2, Delta B.1.617.2, BA.5, XBB.1, and XBB.1.5. To facilitate the study of infections caused by different variants of SARS-CoV-2 PsV, we have developed a HEK-293T cell line expressing mCherry and human angiotensin converting enzyme 2 (ACE2). To validate whether different SARS-CoV-2 PsV variants can be used for neutralization assays, we employed serum from rats immunized with the PF-D-Trimer protein vaccine to investigate its inhibitory effect on the infectivity of various SARS-CoV-2 PsV variants. According to our observations, the XBB variant, particularly XBB.1.5, exhibits stronger immune evasion capabilities than the prototype SARS-CoV-2, Delta B.1.617.2, and BA.5 PsV variants. Hence, utilizing the neutralization test, this study has the capability to forecast the effectiveness in preventing future SARS-CoV-2 variants infections.

1. Introduction

The COVID-19 pandemic has posed a significant threat to global life security, with over 771 million infections and 6.9 million fatalities recorded as of October 18, 2023. This disruption has profoundly affected the daily lives of people worldwide and instigated an unprecedented disruption to the global economy. Vaccines and therapeutic monoclonal antibodies were rapidly developed in response [1,2]. As of October 15, 2023, a total of 13.5 billion vaccine doses have been administered globally.

SARS-CoV-2, a single-stranded RNA virus, exhibits a propensity for rapid mutation due to its replication process. This allows for the

* Corresponding author. National "111" Center for Cellular Regulation and Molecular Pharmaceutics, Key Laboratory of Fermentation Engineering (Ministry of Education), Hubei Provincial Cooperative Innovation Center of Industrial Fermentation, College of Bioengineering, Hubei University of Technology, Wuhan, China.
E-mail address: liubl@hbut.edu.cn (B. Liu).

https://doi.org/10.1016/j.heliyon.2024.e29939
Received 5 March 2024; Received in revised form 18 March 2024; Accepted 17 April 2024
Available online 18 April 2024

assembly of numerous progeny virus particles in a short period, contributing to its rapid transmission and evolution. Recombination also plays a vital role in SARS-CoV-2 evolution. During mixed infections, coronaviruses can fuse with each other, with genetic recombination acting as a crucial pathway for their evolutionary adaptation. Through recombination, coronaviruses can accumulate multiple mutations in a single event, potentially increasing viral transmissibility and immune evasion [3–6].

The virus has undergone an evolutionary path, progressing from Wuhan-Hu-1 through variants such as B.1, Alpha, Beta, Gamma, and Delta. These variants have developed a greater ability to evade the immune system [7]. The Omicron variant, with its significant immune evasion capability, has been associated with an increase in breakthrough infections [8]. Since late 2022, the Omicron subvariant XBB.1.5 has become the dominant lineage of SARS-CoV-2. Key amino acid mutations in its spike (S) protein contribute to the XBB variant's significant immune escape capability [9]. Compared to the XBB.1 variant, the receptor-binding domain (RBD) of the XBB.1.5 variant's S protein shows a single mutation (S486P). This mutation can affect the virus's transmission capability by modulating the efficiency of viral cell entry and potentially alter its susceptibility to antibody-mediated neutralization [10].

Despite its potential for research, working with live SARS-CoV-2 presents challenges due to its contagiousness and virulence, requiring handling in biosafety level 3 (BSL3) facilities [11]. This requirement can hinder and delay the development of effective antiviral candidates. Fortunately, PsVs effectively mitigate this constraint. PsVs can infect susceptible cells but only undergo a single replication cycle within the host, making them generally safer and easier to use for experimental purposes compared to the wild-type (WT) virus [12,13]. Importantly, the structural conformation of pseudoviral surface proteins closely resembles that of natural viral proteins, facilitating efficient invasion of host cells [14]. Therefore, producing SARS-CoV-2 PsV particles is crucial in the absence of live SARS-CoV-2 virus [15]. Once obtained, PsV particles of the SARS-CoV-2 S protein can be used for neutralizing antibody detection, further evaluating the neutralizing ability of antibodies in serum samples from COVID-19 patients [16].

In this study, we developed a dual-reporter PsV system based on an HIV vector to investigate the entry process of SARS-CoV-2. This system simultaneously expresses ZsGreen1 and Fluc, enabling convenient observation and analysis of viral infection. Additionally, the PsV system was designed to analyze the effects of S protein mutations in different SARS-CoV-2 variants on target cell infection.

We utilized a lentivirus (LV), also based on an HIV vector, expressing both human angiotensin converting enzyme 2 (ACE2) and mCherry. These ACE2-mCherry-293T cells, constructed through lentiviral transduction, served as target cells for SARS-CoV-2 variant infection.

To evaluate the protective efficacy of the PF-D-Trimer protein vaccine against various PsV variants, we immunized rats with this vaccine. PF-D-Trimer is a subunit SARS-CoV-2 vaccine candidate containing the recombinant S-glycoprotein from the Delta variant in its prefusion form, trimerized by fusion with a proprietary Trimer Domain (TD). TD is a fragment from the hemagglutinin long alpha helix linked by disulfide bonds, mimicking its natural intermolecular proximity in the heptad repeat. It has been successfully used to stabilize, trimerize, express, and purify soluble SARS-CoV-2 RBD and S1, as well as influenza hemagglutinin H7. As previously demonstrated, PF-D-Trimer induces a strong immune response, generating circulating and neutralizing antibodies against the original WA1 virus, the Delta variant, and different Omicron variants. These results support our vaccine strategy of using the Delta variant S protein as an antigen [17]. To assess the neutralization effect, we analyzed serum samples from vaccinated rats for changes in the neutralization inhibition rate against various PsV variants.

2. Materials and methods

2.1. Animals and immunization

6-week-old Sprague-Dawley rats were acquired from the Hubei Laboratory Research Centre. In a regulated setting with a 12-h cycle of light and darkness, animals were provided unrestricted availability to water and food. Approval number 2021018 was granted by the Laboratory Animal Ethics Review Committee of Hubei University of Technology for the *in vivo* experiments.

The immunization of Sprague-Dawley rats was done via intramuscular (IM) injection using 30 μg of PF-D-Trimer along with 375 μg of alum and 0.75 mg of CpG 1018 as an adjuvant. The total injection volume of the formulated vaccines was 500 μL per IM dose. The administration of three intramuscular doses took place on Day 0, Day 22, and Day 43. The sera were collected at Day 71.

2.2. Plasmids

The amino acid and nucleotide sequences of the S protein of each variant, with 19 amino acids deleted from the C-terminus, are provided in the supplementary information. Additionally, the nucleotide sequences of the S protein for different variants were synthesized using whole-gene synthesis technology. Finally, the S proteins were cloned into the pCMV eukaryotic expression vector after PCR amplification with primers from Supplementary Table S1. Specifically, this experiment used the 2 × Phanta Flash Master Mix high-fidelity enzyme (Vazyme) and added forward primer and reverse primer for PCR amplification of different S protein nucleotide sequences. During the process, the *Kpn*I and *Xba*I restriction endonucleases (New England Biolabs) were used for double-digestion of the pCMV vector to obtain a linear vector. The PCR amplification products and the double-digest products were loaded into separate wells of a 0.1 % agarose gel for electrophoresis. The FastPure Gel DNA Extraction Mini Kit (Vazyme) was used for gel extraction of the desired PCR product bands and the linearized vector bands. The DNA concentration of the gel-extracted products was measured using Qubit (Thermo Fisher Scientific). According to the instructions of the ClonExpress II One Step Cloning Kit (Vazyme), corresponding volumes were added for cloning. Subsequently, transformation and colony PCR sequencing were performed to obtain the recombinant plasmid pCMV-SARS-CoV-2 S. The construction process of the SARS-CoV-2 PsV transfer plasmid is as follows: the Fluc fragment from the pLVX-CMV-Fluc-T2A-GFP-Puro plasmid was PCR amplified using forward and reverse primers (Supplementary Table S2).

Simultaneously, the pLVX-EF1α-IRES-ZsGreen1 plasmid was digested with *Eco*RI and *Bam*HI restriction enzymes to obtain a linearized vector. Subsequently, the Fluc fragment was cloned into the linearized vector to generate the recombinant plasmid pLVX-EF1α-FLuc-IRES-ZsGreen1. This plasmid serves as the transfer plasmid for the SARS-CoV-2 PsV RNA genome and expresses reporter genes for infectivity analysis. The human ACE2 gene, synthesized by GenScript Biotech, China, was PCR amplified using forward and reverse primers (Supplementary Table S2) and then cloned into the linearized vector obtained by double digestion of the pLVX-CMV-MCS-SV40-mCherry plasmid (Hedgehog Bioscience and Technology) with *Xho*I and *Avr*II, ultimately yielding the recombinant plasmid pLVX-CMV-ACE2-SV40-mCherry. The PCR, double digestion, and cloning steps are consistent with those used in the construction of the pCMV-SARS-CoV-2 S plasmid. This plasmid functions as the transfer plasmid for the lentivirus (LV) and expresses ACE2, the receptor for SARS-CoV-2 entry, on target cells. Finally, the pMD2. G and psPAX2 plasmids, expressing LV envelope proteins, were obtained from Miaoling Biology.

2.3. Cell culture

The HEK-293T (human embryonic kidney) cell was cultured in high glucose Dulbecco's modified Eagle medium (DMEM, Livning, China) containing 10 % fetal bovine serum (FBS, Bio-Channel, China) in a 5 % CO_2 environment at 37 °C and passaged every 3 days. The Huh7 (hepatocytes) cells, the SW620 (colorectal adenocarcinoma) cells, the HCT116 (colorectal carcinoma) cells, and the A549 (alveolar epithelial) cells were cultured in DMEM/F-12 (Livning, China) containing 10 % FBS in a 5 % CO_2 environment at 37 °C and passaged every 3 days. All of the above cells were purchased from Procell.

2.4. Generation of human ACE2 over-expressing cells

HEK-293T cells were seeded in a 10 cm dish at a density of 1×10^6 cells/mL [18]. Upon reaching 80 % confluence, the cells were transfected with a mixture of 12 μg pLVX-CMV-ACE2-SV40-mCherry, 6 μg psPAX2, and 3 μg pMD2.G plasmids using PEI MAX [19]. Supernatants were collected 48 and 72 h post-transfection, centrifuged at 3000×*g* for 5 min at 4 °C to remove debris, and then transferred to new tubes. The lentivirus particles were concentrated using a 100 kDa MWCO filter [20] and aliquoted for storage at −80 °C.

To generate the ACE2-mCherry-293T cell line, HEK-293T cells were seeded in a 96-well plate at 2×10^4 cells/well and transduced overnight with the concentrated lentivirus particles and 6–8 μg/mL polybrene. The next day, the culture medium containing LV was discarded, and transduced cells were incubated with fresh DMEM for 48–72 h mCherry expression was monitored using fluorescence microscopy. Single cells exhibiting mCherry fluorescence were isolated after trypsinization and seeded in a 96-well plate at 1–2 cells per well. Single-cell clones were expanded and cultured. The transduced HEK-293T cells were observed daily, and the medium was changed every three days [21].

2.5. Preparation of COVID-19 PsVs

To generate SARS-CoV-2 PsVs, a three-plasmid approach was employed, utilizing the lentiviral Gag/Pol-containing vector psPAX2, an HIV-based LV packaging vector, to supply the capsid for PsV. The RNA genome for PsV was provided by using the plasmid pLVX-EF1α-FLuc-IRES-ZsGreen1, which included two reporter genes, namely ZsGreen1 and Fluc. PsV is provided with S glycoprotein by using the third plasmid containing the envelope fragment of SARS-CoV-2, named pCMV-SARS-CoV-2 S. The polyetherimide (PEI) MAX transfection reagent was used to co-transfect HEK-293T cells with these three plasmids. ZsGreen1 was utilized for assessing the transfection effectiveness. After mixing the plasmid and transfection reagent, the mixture was transfected into HEK-293T cells. Supernatants were collected from 0 to 48 h and 48–72 h separately into sterile centrifuge tubes. The tubes were then centrifuged at 3000×*g* for 5 min at 4 °C. The supernatants containing PsV particles were transferred to new centrifuge tubes after filtration through a 0.45 μm filter. Finally, the filtered supernatants were aliquoted into sterile EP tubes and stored at −80 °C.

2.6. Pseudotyped virus infection assays

ACE2-mCherry-293T cells (2×10^4 cells/well) were seeded in a 96-well plate and incubated overnight at 37 °C in a 5 % CO_2 incubator one day before infection. The next day, the culture medium was discarded and replaced with a mixture of PsV supernatant (containing 6–8 μg/mL polybrene) and fresh complete medium. The cells were then incubated with the PsV for 12–18 h. Finally, the culture medium was replaced with fresh complete medium. The cells were maintained in culture for an additional 48 h. To measure luciferase activity, 100 μL/well (150 μg/mL) of D-luciferin potassium salt (Beyotime, China) was added to the 96-well plate and co-incubated with cells transduced with different PsV variants for 10 min. Subsequently, RLU (Relative Light Units) values were measured using a Varioskan™ LUX multimode microplate reader (Thermo Fisher Scientific) [22].

2.7. Flow cytometry

For the detection of ACE2 expression, ACE2-mCherry-293T cells, obtained through trypsin digestion, were resuspended in phosphate-buffered saline (PBS) to create a single-cell suspension. These cells were then stained with 5 μL of FITC-labeled anti-ACE2 antibody (Sino Biological) per test and incubated for 30 min at 4 °C. Following three washes with PBS, ACE2 expression was analyzed on a NovoCyte flow cytometer (Agilent NovoCyte 3000). The flow rate of the flow cytometer was 35 μL/min, with the sample loading

speed set at 500–1500 cells per second. Both the FITC and PE fluorescence channels used band-pass filters, corresponding to wavelengths of 530/30 nm and 572/28 nm, respectively, and the laser wavelength used for both fluorescence channels was 488 nm.

To determine the titer of the lentiviral particles, HEK-293T cells were seeded in a 96-well plate at a density of 2×10^4 cells per well in DMEM complete medium supplemented with 6–8 μg/μL of polybrene. Serial dilutions of the lentiviral particles (10 μL per well) were added to each well. After 72 h of incubation, the percentage of mCherry-positive cells was determined by flow cytometry.

PsV titer was determined by first seeding ACE2-mCherry-293T cells in a 96-well plate at a density of 2×10^4 cells per well and incubated overnight. The culture medium was then removed, and 100 μL of PsV supernatant was added to each well. Following 24 h of incubation with the PsV, the cells were cultured in fresh DMEM complete medium. ZsGreen1 expression was quantified by flow cytometry 72 h after infection.

The titration of LV and PsV can be calculated using the same formula. Transduction Units (TU/mL) = F × C × D/V. F: the expression rate of fluorescent reporter genes (ZsGreen1 or mCherry); C: cell number per well on the day of transduction; D: Dilution factor of the virus; V: virus volume [23].

2.8. PsV-based neutralization assay

Following immunization with the Delta B.1.617.2 protein vaccine, the rat sera were incubated at 56 °C for 30 min to inactivate the complement. Subsequently, the sera were diluted at a ratio of 1:80, and then further diluted in a 2-fold serial manner. The diluted sera were mixed with PsV (2×10^4 TU/mL) in 96-well plates, respectively. After resting at 37 °C for 1 h, the mixture of serum and PsV was incubated overnight with ACE2-mCherry-293T cells. Subsequently, the medium was replaced with fresh DMEM complete culture medium, and incubation was continued for 48 h [24]. Chemiluminescence signals were measured using a Varioskan™ LUX multimode microplate reader and expressed as RLU values. The calculation of the inhibition rates for each dilution of the sample is based on the RLU values, using the formula: inhibition rate = [1 - (average RLU of sample - average RLU of cell control)/(average RLU of virus control - average RLU of cell control)] × 100 % [25].

Results were processed using GraphPad Prism 8.0 (GraphPad) and are displayed as means ± standard deviations (SD). Significance thresholds: *p < 0.05, **p < 0.01, ***p < 0.005, and ****p < 0.001.

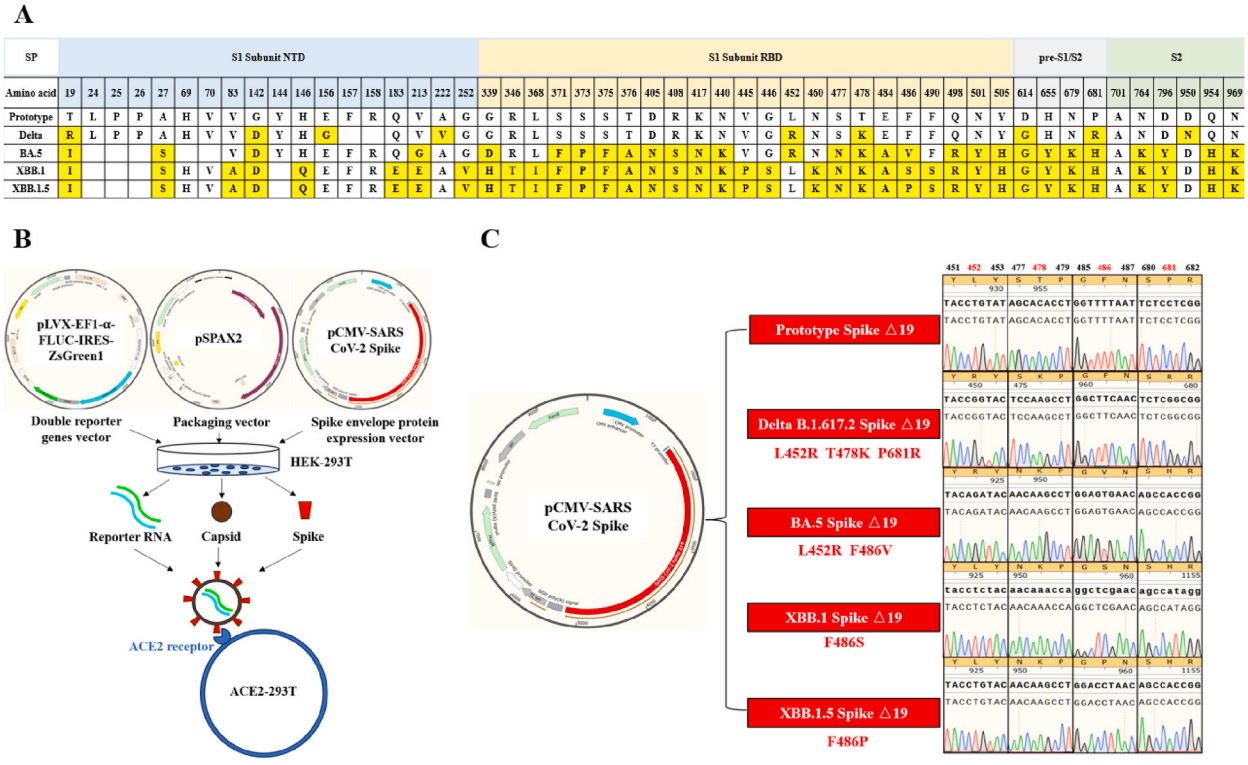

Fig. 1. Production of basic Spike-pseudotyped lentiviral vector. (A) Displaying spike protein mutations of analyzed SARS-CoV-2 PsV variants. Amino acid mutations manifest in various forms: substitutions, deletions (blank squares), and insertions (yellow squares). SP: signal peptide. NTD: N-terminal domain. RBD: receptor-binding domain. (B) Characteristic process for the production of SARS-CoV-2 PsV variants encoding ZsGreen1 and Fluc. (C) Sequence of S protein base of different variants of COVID-19 and display of key amino acid mutation. (For interpretation of the references to color in this figure legend, the reader is referred to the Web version of this article.)

3. Results

3.1. Production of basic S-pseudotyped lentiviral vector

To construct pseudovirus (PsV) envelopes incorporating various SARS-CoV-2 S protein variants, we employed their respective amino acid sequences. Compared to the prototype strain, these variants harbor diverse deletions and mutations (Fig. 1A). PsV production involved co-transfecting HEK-293T cells with three plasmids: pLVX-EF-α-FLuc-IRES-ZsGreen1 (expressing reporter genes), psPAX2 (packaging plasmid), and pCMV-SARS-CoV-2 (variant-specific S protein plasmid). Between 48 and 72 h post-transfection, cells release PsV particles into the supernatant that recognize and infect ACE2-expressing 293T cells (Fig. 1B). To generate PsVs expressing the SARS-CoV-2 S protein, the S gene was incorporated into the pCMV vector, commonly used for envelope protein expression. The functionality of each PsV variant is dictated by its specific pCMV-SARS-CoV-2 S envelope plasmid. Notably, all S proteins in this study lack the C-terminal 19 amino acids, which typically function as a retention signal within the endoplasmic reticulum. Further sequence analysis confirmed the presence of key S protein mutations in each PsV variant (Fig. 1C). These mutations vary in position and nature across different variants. For instance, the Delta B.1.617.2 variant harbors a unique combination of T478K, P681R, and L452R mutations [26]. Similarly, the BA.5 variant possesses two signature mutations, L452R and F486V [27]. Finally, XBB.1.5 emerged from XBB.1 (F486S) through the acquisition of the F486P mutation in the S protein [28].

3.2. Construction and identification of stable ACE2-mCherry-293T cell line

To facilitate efficient transduction of HEK-293T cells by SARS-CoV-2 PsV, we established a stable cell line overexpressing the ACE2 receptor. The ACE2 gene was integrated into the pLVX vector's multiple cloning site (MCS). Additionally, the mCherry fluorescent protein gene was placed under a SV40 promoter, and the puromycin resistance gene under a PGK promoter (Fig. 2A). PCR amplified the ACE2 gene, and the products were inserted into the pLVX-CMV-MCS-SV40-mCherry plasmid through homologous recombination followed by transformation. Successful insertion of the ACE2 fragment was confirmed by colony PCR (Fig. 2C). Co-transfection of three plasmids resulted in lentiviral particles containing the construct. Flow cytometry determined the concentrated lentiviral titer, revealing mCherry positivity upon 10-fold dilution. The calculated transduction units were 3.06×10^8 TU/mL for unexpressed ACE2 and 3.03×10^7 TU/mL for expressed ACE2 (Fig. 2D). HEK-293T cells infected with LV-mCherry and LV-ACE2-mCherry were isolated using limited dilution and seeded in a 96-well plate. Monoclonal cells were imaged on days 7 and 25 using an Operetta High Content

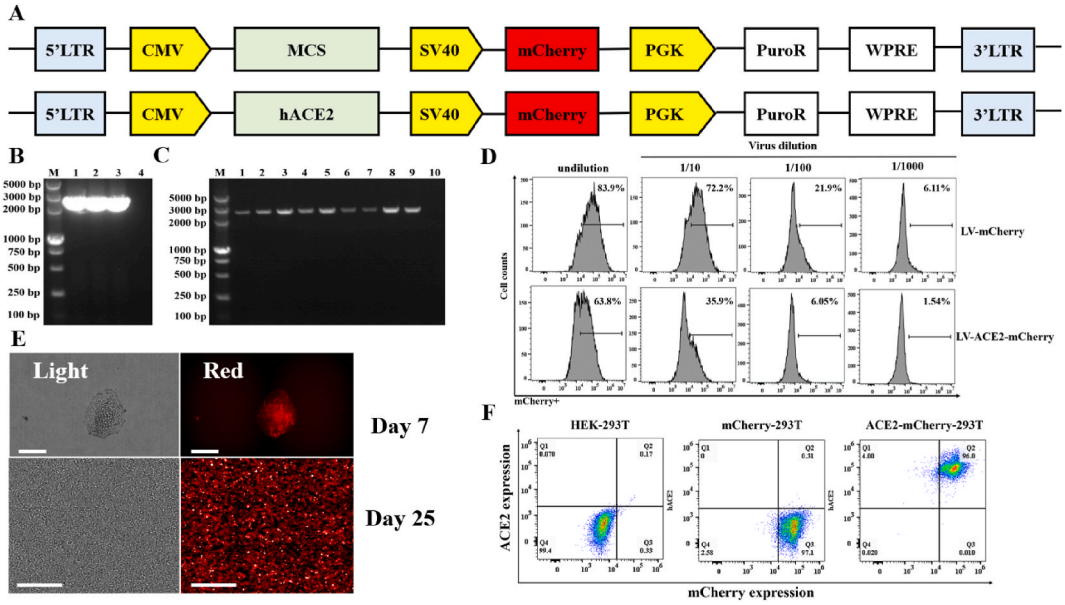

Fig. 2. Construction and identification of stable ACE2-mCherry-293T cell line. (A) Represent the maps for the empty pLVX-CMV-MCS-SV40-mCherry vector backbone and pLVX-CMV-ACE2-SV40-mCherry vector. (B) Agarose gel electrophoresis of PCR for ACE2 fragment. M: DL5000 DNA Marker; Lanes 1–3: ACE2 construct PCR products; Lanes 4: negative control without template. (C) Agarose gel electrophoresis of colony PCR for pLVX-CMV-ACE2-SV40-mCherry recombinant plasmid. M: DL5000 DNA Marker; Lanes 10: negative control without template, others were experimental group samples. (D) The titers of LV-mCherry and LV-mCherry-ACE2 were detected by flow cytometry. (E) Over-expressing ACE2-mCherry single-cell culture from clonal expansion. Operetta High Content Imaging System images show single-cell into a 96-well plate on (day 7) and subsequent expansion (day 25) of ACE2-mCherry-293T previously isolated and cultured inside 6-well plate. Left: brightfield photographs depicting a single cell and the cell after expansion are displayed. Right: mCherry photographs depicting a single cell and the cell after expansion are displayed. The scale bar represents 200 μm (top) and 500 μm (bottom) respectively. (F) ACE2 and mCherry expression of ACE2-mCherry-293T were determined by flow cytometry.

Imaging System (Perkin Elmer) (Fig. 2E). Flow cytometric analysis with FITC anti-human ACE2 antibody confirmed ACE2 expression in mCherry-positive cells, with a double positivity rate of 96 % (Fig. 2F). This stable ACE2-mCherry-HEK-293T cell line was determined to be suitable for further studies involving SARS-CoV-2 PsV infection.

3.3. Dual-reporter SARS CoV-2 PsV production and infectivity

To simplify observation and analysis, a single vector expressing both ZsGreen1 and Fluc was designed (Fig. 3A). SARS-CoV-2 PsVs were generated using a three-plasmid co-transfection approach involving pCMV-SARS-CoV-2 S for S protein expression, psPAX2 as the packaging plasmid, and pLVX-EF1-α-FLuc-IRES-ZsGreen1 as the transfer plasmid. Approximately 80 % of HEK-293T cells expressed fluorescent protein 48–72 h post-transfection, indicating efficient plasmid transduction (Fig. 3B).

To investigate PsV production over time, supernatants from different variants collected at various intervals were used to infect ACE2-mCherry-293T cells. RLU values were higher at 48–72 h compared to 0–48 h, with the XBB variant displaying the highest RLU value (Fig. 3C). Further evaluation of PsV transduction efficiency using ACE2-mCherry-293T cells revealed readily observable infection using an Operetta High-Content Imaging System (Fig. 3D). Flow cytometry analysis quantified ZsGreen1 reporter gene expression, with the positive control SARS-CoV PsV showing the highest GFP expression (40.08 %), followed by XBB.1 (10.70 %) and XBB.1.5 (9.65 %). Other variants exhibited lower expression rates (5.67 %–10.30 %). PsV variant concentrations ranged from 1.70×10^4 TU/mL to 3.21×10^4 TU/mL.

3.4. Various cell lines exhibited varying levels of susceptibility to PsV variants

Afterwards, we assessed if SARS-CoV-2 PsV had the capability to infect cell lines derived from the human kidney, liver, and colon. VSV-G PsV served as the experimental group for comparison purposes. The measurement of Fluc activity was conducted at 72 h post-infection. As anticipated, VSV-G PsV efficiently transduced all types of cells. The SARS-CoV-2 PsV variants show higher RLU values when infecting ACE2-mCherry-293T cells and Huh7 cells compared to HEK-293T cells, HCT116, and A549 cell lines, indicating that different cell types have varying degrees of sensitivity to these PsV variants. In addition, we noticed a pattern where, except for SW620 cells, SARS-CoV PsV generated greater RLU values in comparison to SARS-CoV-2 PsV while infecting different cells. This indicates the possibility of distinct mechanisms of cell entry mediated by S protein, distinguishing between SARS-CoV-2 and SARS-CoV.

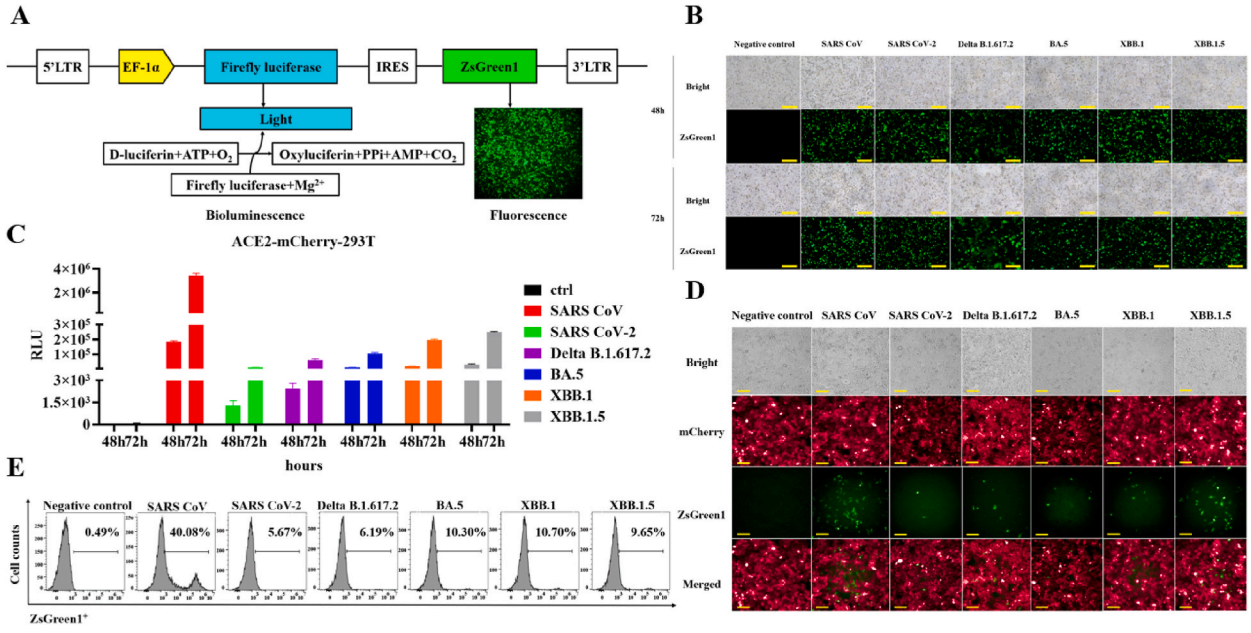

Fig. 3. Dual-reporter SARS CoV-2 PsV production and infectivity. (A) The illustration represents a model of the transfer plasmid for the SARS-CoV-2 PsV expressing dual reporter genes. Firefly luciferase-IRES-ZsGreen1, dual-reporter genes. (B) PsV three plasmids were co-transfected into 293T cells. The expression of ZsGreen1 fluorescence was observed using an inverted fluorescence microscope at different time points (Scar bar, 500 μm). Unifected HEK-293T as negative control. (C) The RLU values of ACE2-mCherry-293T cells infected with collected SARS-CoV-2 PsV variants at different time points were measured using microplate reader. (D) Operetta High Content Imaging System images show that SARS-CoV-2 PsV (green) infection in ACE2-mCherry-293T cells (mCherry) (Scar bar, 100 μm). SARS-CoV PsV as positive control. (E) Titration determination of SARS-CoV-2 PsV different variants by flow cytometry. The results of SARS-CoV PsV infection in ACE2-mCherry-293T cells were used as a positive control and untransduced ACE2-293T-mCherry as a negative control. (For interpretation of the references to color in this figure legend, the reader is referred to the Web version of this article.)

3.5. Reduced neutralization of rat serum immunized with PF-D-trimer against the XBB variants

To evaluate the neutralization potential of different PsV variants against vaccinated serum, we exposed SARS-CoV-2 prototype, Delta B.1.617.2, BA.5, XBB.1, and XBB.1.5 to varying dilutions of serum from two rats immunized with the PF-D-Trimer vaccine. Subsequently, ACE2-mCherry-293T cells were added for analysis. Quantifiable neutralization inhibition rates were determined by analyzing luciferase intensity values.

Both rat sera exhibited differential inhibitory effects against various PsVs and dilutions. Rat 1 serum diluted between 1:80 and 1:2560 demonstrated a stronger inhibitory effect on prototype, Delta B.1.617.2, and BA.5 compared to XBB variants (Fig. 5A). Similarly, rat 2 serum at dilutions ranging from 1:80 to 1:640 showed a higher inhibition rate against the prototype, Delta B.1.617.2, and BA.5 compared to XBB.1 and XBB.1.5 (Fig. 5B). Interestingly, rat 2 serum displayed inhibitory activity against XBB.1, but not XBB.1.5, at dilutions from 1:1280 to 1:5120, possibly due to individual animal variations. Nonetheless, both sera significantly neutralized XBB.1.5 at all dilutions. These findings suggest that mutations within XBB variants, particularly in XBB.1.5, enable them to partially evade neutralizing antibodies generated by the PF-D-Trimer vaccine.

4. Discussion

PsVs are valuable tools for studying coronavirus entry processes and developing antiviral drugs, and their production in BSL2 facilities offers significant safety advantages [29]. The HIV-1 lentiviral system is a popular choice for generating SARS-CoV-2 PsVs, typically involving co-transfection of 2–3 plasmids into host cells [30,31]. This system consists of three crucial components: a packaging vector, a plasmid carrying a reporter gene, and another encoding the viral envelope protein [32].

In this study, we utilized the same lentiviral system to address two key issues. First, we integrated the ACE2 gene into the transfer plasmid, creating the pLVX-CMV-ACE2-SV40-mCherry plasmid. Co-transfection of this plasmid with psPAX2 and pMD2. G into HEK-293T cells produced a lentivirus overexpressing ACE2 (Fig. 2). This lentivirus can transduce various cell types, generating stable ACE2-expressing cell lines—valuable tools for studying coronavirus target cell invasion [33].

Second, we incorporated the Fluc and ZsGreen1 reporter genes into the transfer plasmid, creating pLVX-EF1-α-FLuc-IRES-ZsGreen1. Additionally, the S gene was inserted into a separate vector to create the pCMV-SARS-CoV-2 S envelope plasmid. Co-transfection with psPAX2 into HEK-293T cells generated a PsV overexpressing Fluc, ZsGreen1, and the S protein, enabling accurate and convenient quantitative analysis (Fig. 3).

Initially, we used the non-truncated S gene to package the SARS-CoV-2 PsV. However, this resulted in low green fluorescence expression and RLU values in infected ACE2-293T cells. By introducing a specific truncation mutation, we achieved a remarkable 100-fold increase in PsV titers, reaching approximately 1×10^4 TU/mL compared to 1×10^2 TU/mL with the wild-type S protein [34]. For further optimization, we selectively deleted the final 19 amino acids from the S protein's cytoplasmic tail, targeting the endoplasmic reticulum retention signal [35–37]. This modification aligned with previous literature and resulted in PsV titers ranging from 1 to 3×10^4 TU/mL for the five SARS-CoV-2 variants tested, consistent with published findings.

These are the key findings from the study. First, enhanced PsV production: Following co-transfection with PsV plasmids, peak viral particle production occurred at 48–72 h post-transfection, as indicated by higher RLU values in the collected supernatant (Fig. 3C). This suggests efficient PsV synthesis during this timeframe. Second, variant-dependent RLU values: Among different PsVs infecting ACE2-mCherry-293T cells under identical conditions, RLU values increased in the following order: SARS-CoV-2 prototype, Delta B.1.617.2, BA.5, XBB.1, XBB.1.5 (Fig. 3C). This trend aligns with the heightened infectivity observed in recent Omicron subvariants, particularly XBB [38]. The discrepancy could be attributed to S protein mutations in different SARS-CoV-2 PsVs, potentially enhancing viral ability to invade target cells during evolution. Third, SARS-CoV PsV displayed higher RLU values in ACE2-mCherry-293T cells compared to SARS-CoV-2 (Fig. 3C). While both utilize ACE2 for entry [39], their S protein sequences differ. Viral entry starts with S protein binding to the cell surface ACE2 receptor, followed by endocytosis and fusion with the cell or lysosomal membrane [40]. Importantly, S protein mutations can lead to variants with altered cellular tropism and virulence [41]. Finally, cell line susceptibility:

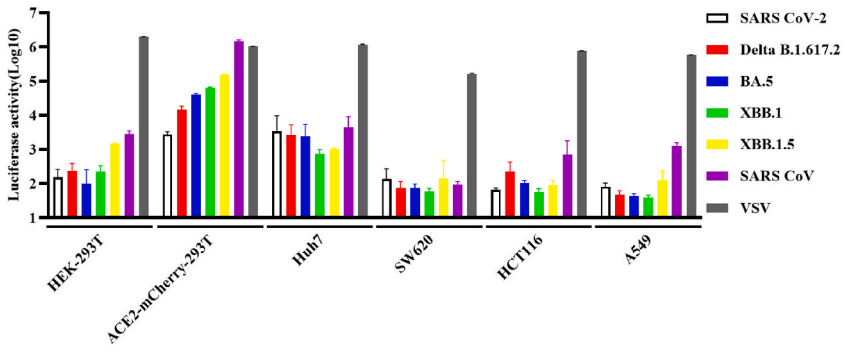

Fig. 4. Various cell lines exhibited varying levels of susceptibility to PsV variants. Bioluminescence detection of SARS-CoV-2 PsV different variants infectivity to kidney, liver, lung, and colon-derived cell lines.

Using the PsV system, we investigated the sensitivity of different cell lines to PsV. Huh7 cells exhibited the highest susceptibility to various PsVs (Fig. 4), consistent with previous findings [42]. This suggests a potential role for proteins like ACE2 or TMPRSS2 in SARS-CoV-2 cellular entry [43]. While ACE2-positive cells are prevalent in the lungs of COVID-19 patients, ACE2-negative cells susceptible to infection have also been identified, suggesting an alternative, ACE2-independent entry mechanism [44]. Understanding the effects of SARS-CoV-2 across various cell types is crucial for elucidating the pathobiology and clinical features of COVID-19.

The ultimate goal of the PsV system we have developed is its application in neutralization tests. Our study revealed that serum samples from rats vaccinated with the PF-D-Trimer exhibited varying degrees of neutralizing activity against different PsV variants, particularly showing lower inhibition rates against the XBB lineage (Fig. 5). This observation aligns with previously reported conclusions that the XBB lineage possesses a notable ability to evade neutralizing antibodies, primarily due to its distinct constellation of mutations within the S protein [45]. Furthermore, these findings suggest that, when subjected to equivalent conditions of serum antibody neutralization, the XBB lineage exhibits notably diminished neutralization activity and protective immunity against PF-D-Trimer compared to the SARS-CoV-2 prototype, Delta B.1.617.2, and BA.5. This discrepancy can be attributed to the additional mutation at residue S486, where it is substituted with P486 in the XBB.1.5 variant. Consequently, this mutation allows for the restoration of higher receptor affinity while simultaneously maintaining a comparable level of immune evasion.

Upon reviewing the entire study, we recognized several shortcomings in our research. Firstly, the titer of SARS-CoV-2 PsV variants prepared in this study needs to be optimized. This could be achieved by refining the transfection ratios of the three plasmids, or by adding different signal peptides to the N-terminus of the S protein to enhance the PsV' ability to invade target cells. Secondly, the five SARS-CoV-2 PsV variants used in this study represent only a small fraction of all coronavirus variants. We plan to expand the variety of PsV variants in future studies to enrich the dataset in the field of SARS-CoV-2 PsV. Thirdly, the serum produced by immunizing rats with the PF-D-Trimer protein vaccine was used in neutralization tests. Producing and purifying this protein vaccine, as well as its functional validation is quite challenging, leading to a limited number of animals and species used in related neutralization experiments. We aim to further optimize the production and purification conditions of the protein vaccine to meet the requirements for more animal model neutralization tests. In addition to PF-D-Trimer, we are also designing SARS-CoV-2 vaccines based on the S proteins of different variants in order to explore their protective capabilities against different SARS-CoV-2 strains through neutralization tests.

In conclusion, the continuous mutation of the SARS-CoV-2 virus poses a significant threat to public health. The antibodies produced from natural infections with SARS-CoV-2 variants are no longer sufficient to protect individuals from further infections with new variants of the virus. Moreover, the production speed of SARS-CoV-2 vaccines is far slower than the rate of virus mutation. There is an immediate necessity to conduct a thorough evaluation of the protective immune responses exhibited by individuals who have been infected, particularly against the strains of the virus currently in circulation, with the aim of accurately predict the likelihood of future

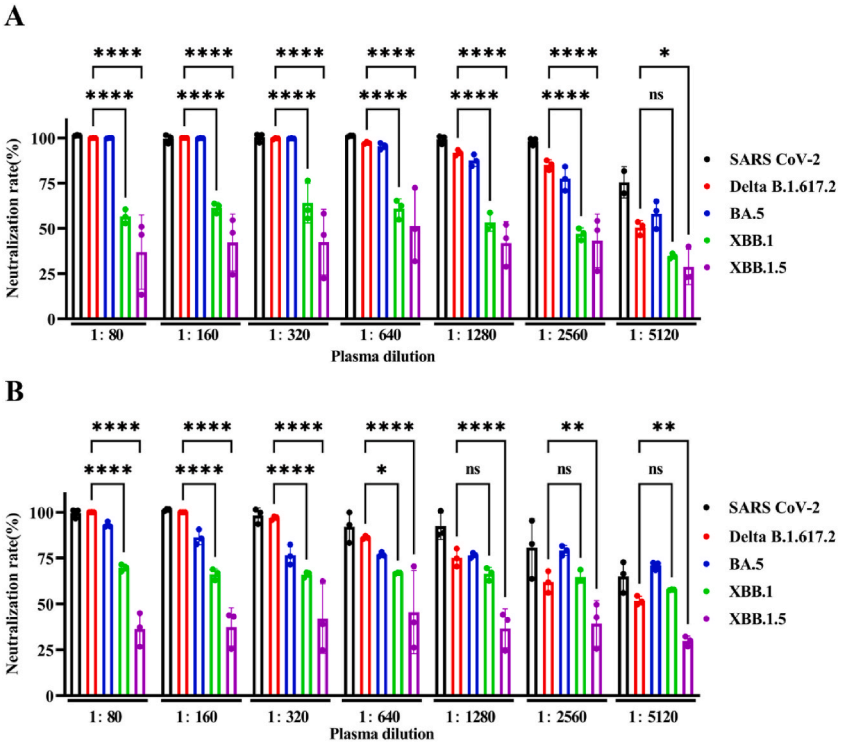

Fig. 5. Reduced neutralization of rat serum immunized with PF-D-Trimer against the XBB Variants. Pseudotypes were incubated with two-fold serially diluted serum of different rats for 60 min at 37 °C, and then were incubated onto ACE2-mCherry-293T cells. Upon 72 h, cells activity of Fluc was analyzed. Neutralizing rate was quantitatively analyzed using Graphpad.

infection.

Funding statement

The study was supported by the National Natural Science Foundation of China (82001758).

Data availability

Data will be made available on request.

CRediT authorship contribution statement

Haixiao Duan: Writing – review & editing, Writing – original draft, Methodology, Formal analysis, Data curation, Conceptualization. **Ershuai Zhang:** Investigation, Formal analysis, Data curation. **Ge Ren:** Investigation, Formal analysis, Data curation. **Yining Cheng:** Methodology, Investigation, Data curation. **Binfeng Yang:** Validation, Investigation. **Lirong Liu:** Validation, Investigation. **Normand Jolicoeur:** Validation, Resources, Methodology, Investigation, Conceptualization, Writing – review & editing. **Han Hu:** Writing – review & editing, Methodology, Formal analysis. **Yan Xu:** Writing – review & editing, Visualization, Resources, Methodology, Investigation, Conceptualization. **Binlei Liu:** Supervision, Project administration, Funding acquisition, Conceptualization, Writing – review & editing.

Declaration of competing interest

The authors declare that they have no known competing financial interests or personal relationships that could have appeared to influence the work reported in this paper.

Acknowledgements

The authors acknowledge the kind helps of Yujie Guo and Jinhu Zhou during this study.

Appendix A. Supplementary data

Supplementary data to this article can be found online at https://doi.org/10.1016/j.heliyon.2024.e29939.

References

[1] Q. Wang, S. Iketani, Z. Li, L. Liu, Y. Guo, Y. Huang, A.D. Bowen, M. Liu, M. Wang, J. Yu, R. Valdez, A.S. Lauring, Z. Sheng, H.H. Wang, A. Gordon, L. Liu, D. D. Ho, Alarming antibody evasion properties of rising SARS-CoV-2 BQ and XBB subvariants, Cell 186 (2023) 279–286.e8, https://doi.org/10.1016/j.cell.2022.12.018.

[2] S. Zhao, S. Hu, X. Zhou, S. Song, Q. Wang, H. Zheng, Y. Zhang, Z. Hou, The prevalence, features, influencing factors, and solutions for COVID-19 vaccine misinformation: systematic review, JMIR Public Health Surveill. 9 (2023) e40201, https://doi.org/10.2196/40201.

[3] N. He, Rapid evolution of the COVID-19 pandemic calls for a unified public health response, BioSci. Trends 15 (2021) 196–200, https://doi.org/10.5582/bst.2021.01261.

[4] X. Li, E.E. Giorgi, M.H. Marichannegowda, B. Foley, C. Xiao, X.P. Kong, Y. Chen, S. Gnanakaran, B. Korber, F. Gao, Emergence of SARS-CoV-2 through recombination and strong purifying selection, Sci. Adv. 6 (2020) eabb9153, https://doi.org/10.1126/sciadv.abb9153.

[5] S. Lytras, J. Hughes, D. Martin, P. Swanepoel, A. de Klerk, R. Lourens, S.L. Kosakovsky Pond, W. Xia, X. Jiang, D.L. Robertson, Exploring the natural origins of SARS-CoV-2 in the light of recombination, Genome Biol. Evol. 14 (2022) evac018, https://doi.org/10.1093/gbe/evac018.

[6] J. Ou, W. Lan, X. Wu, T. Zhao, B. Duan, P. Yang, Y. Ren, L. Quan, W. Zhao, D. Seto, J. Chodosh, Z. Luo, J. Wu, Q. Zhang, Tracking SARS-CoV-2 Omicron diverse S gene mutations identifies multiple inter-variant recombination events, Signal Transduct. Targeted Ther. 7 (2022) 138, https://doi.org/10.1038/s41392-022-00992-2.

[7] H. Que, L. Chen, X. Wei, SARS-CoV-2 variants, immune escape, COVID-19 vaccine, and therapeutic strategies, Sci. China Life Sci. 66 (2023) 406–410, https://doi.org/10.1007/s11427-021-2164-6.

[8] V. Di Lego, M. Sánchez-Romero, A. Prskawetz, The impact of COVID-19 vaccines on the Case Fatality Rate: the importance of monitoring breakthrough infections, Int. J. Infect. Dis. 119 (2022) 178–183, https://doi.org/10.1016/j.ijid.2022.03.059.

[9] I. Nehlmeier, A. Kempf, P. Arora, A. Cossmann, A. Dopfer-Jablonka, M.V. Stankov, S.R. Schulz, H.M. Jäck, G.M.N. Behrens, S. Pöhlmann, M. Hoffmann, Host cell entry and neutralisation sensitivity of the SARS-CoV-2 XBB.1.16 lineage, Cell. Mol. Immunol. 20 (2023) 969–971, https://doi.org/10.1038/s41423-023-01030-z.

[10] M. Hoffmann, P. Arora, I. Nehlmeier, A. Kempf, A. Cossmann, S.R. Schulz, G. Morillas Ramos, L.A. Manthey, H.M. Jäck, G.M.N. Behrens, S. Pöhlmann, Profound neutralization evasion and augmented host cell entry are hallmarks of the fast-spreading SARS-CoV-2 lineage XBB.1.5, Cell. Mol. Immunol. 20 (2023) 419–422, https://doi.org/10.1038/s41423-023-00988-0.

[11] J. Nie, Q. Li, J. Wu, C. Zhao, H. Hao, H. Liu, L. Zhang, L. Nie, H. Qin, M. Wang, Q. Lu, X. Li, Q. Sun, J. Liu, C. Fan, W. Huang, M. Xu, Y. Wang, Quantification of SARS-CoV-2 neutralizing antibody by a pseudotyped virus-based assay, Nat. Protoc. 15 (2020) 3699–3715, https://doi.org/10.1038/s41596-020-0394-5, 10.1038/s41596-020-0394-5.

[12] J.A. Cruz-Cardenas, M. Gutierrez, A. López-Arredondo, J.E. Castañeda-Delgado, A. Rojas-Martinez, Y. Nakamura, J.A. Enciso-Moreno, L.A. Palomares, M.E. G. Brunck, A pseudovirus-based platform to measure neutralizing antibodies in Mexico using SARS-CoV-2 as proof-of-concept, Sci. Rep. 12 (2022) 17966, https://doi.org/10.1038/s41598-022-22921-7.

[13] J. Yu, Z. Li, X. He, M.S. Gebre, E.A. Bondzie, H. Wan, C. Jacob-Dolan, D.R. Martinez, J.P. Nkolola, R.S. Baric, D.H. Barouch, Deletion of the SARS-CoV-2 S cytoplasmic tail increases infectivity in pseudovirus neutralization assays, J. Virol. 95 (2021) e00044, https://doi.org/10.1128/JVI.00044-21.
[14] Y. Lu, J. Wang, Q. Li, H. Hu, J. Lu, Z. Chen, Advances in neutralization assays for SARS-CoV-2, Scand. J. Immunol. 94 (2021) 224–238, https://doi.org/10.1111/sji.13088.
[15] P. Yang, Y. Yang, Y. Wu, C. Huang, Y. Ding, X. Wang, S. Wang, An optimized and robust SARS-CoV-2 pseudovirus system for viral entry research, J. Virol. Methods 295 (2021) 114221, https://doi.org/10.1016/j.jviromet.2021.114221.
[16] A.M.K. Tolah, S.S. Sohrab, K.M.K. Tolah, A.M. Hassan, S.A. El-Kafrawy, E.I. Azhar, Evaluation of a pseudovirus neutralization assay for SARS-CoV-2 and correlation with live virus-based micro neutralization assay, Diagnostics 11 (2021) 994, https://doi.org/10.3390/diagnostics11060994.
[17] Z. Zhang, J. Zhou, P. Ni, B. Hu, N. Jolicoeur, S. Deng, Q. Xiao, Q. He, G. Li, Y. Xia, M. Liu, C. Wang, Z. Fang, N. Xia, Z.R. Zhang, B. Zhang, K. Cai, Y. Xu, B. Liu, PF-D-Trimer, a protective SARS-CoV-2 subunit vaccine: immunogenicity and application, NPJ Vaccines 8 (2023) 38, https://doi.org/10.1038/s41541-023-00636-8.
[18] C. Chu, A. Xin, Y. Zhou, Y. Zhang, A simple protocol for producing high-titer LV, Acta Biochim. Biophys. Sin. 45 (2013) 1079–1082, https://doi.org/10.1093/abbs/gmt112.
[19] W. Jiang, R. Hua, M. Wei, C. Li, Z. Qiu, X. Yang, C. Zhang, An optimized method for high-titer LV preparations without ultracentrifugation, Sci. Rep. 5 (2015) 13875, https://doi.org/10.1038/srep13875.
[20] C. Perry, N. Mujahid, Y. Takeuchi, A.C.M.E. Rayat, Insights into product and process related challenges of lentiviral vector bioprocessing, Biotechnol. Bioeng. (2023), https://doi.org/10.1002/bit.28498.
[21] H. Hu, Z. Zhang, R. Wang, Y. Wang, J. Jin, L. Cai, J. Yang, H. Duan, Z. Wu, Z. Fang, B. Liu, BGC823 cell line with the stable expression of iRFP720 retains its primary properties with promising fluorescence imaging ability, DNA Cell Biol. 39 (2020) 900–908, https://doi.org/10.1089/dna.2019.5057.
[22] J. Hu, C. He, Q. Gao, G. Zhang, X. Cao, Q. Long, H. Deng, L. Huang, J. Chen, K. Wang, N. Tang, A. Huang, D614G Mutation of SARS-CoV-2 S Protein Enhances Viral Infectivity, 2020, https://doi.org/10.1101/2020.06.20.161323. PPR:PPR178509.
[23] C. Su, K. Ding, J. Xu, J. Wu, J. Liu, J. Shen, H. Zhou, H. Liu, Preparation and application of chikungunya pseudovirus containing double reporter genes, Sci. Rep. 12 (2022) 9844, https://doi.org/10.1038/s41598-022-13230-0.
[24] M.C. Johnson, T.D. Lyddon, R. Suarez, B. Salcedo, M. LePique, M. Graham, C. Ricana, C. Robinson, D.G. Ritter, Optimized pseudotyping conditions for the SARS-COV-2 S glycoprotein, J. Virol. 94 (2020) e01062, https://doi.org/10.1128/JVI.01062-20.
[25] J. Nie, Q. Li, J. Wu, C. Zhao, H. Hao, H. Liu, L. Zhang, L. Nie, H. Qin, M. Wang, Q. Lu, X. Li, Q. Sun, J. Liu, C. Fan, W. Huang, M. Xu, Y. Wang, Quantification of SARS-CoV-2 neutralizing antibody by a pseudotyped virus-based assay, Nat. Protoc. 15 (2020) 3699–3715, https://doi.org/10.1038/s41596-020-0394-5.
[26] M Dhawan, A Sharma, N Priyanka, et al., Delta variant (B. 1.617. 2) of SARS-CoV-2: Mutations, impact, challenges and possible solutions, Hum Vaccin Immunother 18 (2022) 2068883, https://doi.org/10.1080/21645515.2022.2068883.
[27] A. Tuekprakhon, R. Nutalai, A. Dijokaite-Guraliuc, D. Zhou, H.M. Ginn, M. Selvaraj, C. Liu, A.J. Mentzer, P. Supasa, H.M.E. Duyvesteyn, R. Das, D. Skelly, T. G. Ritter, A. Amini, S. Bibi, S. Adele, S.A. Johnson, B. Constantinides, H. Webster, N. Temperton, P. Klenerman, E. Barnes, S.J. Dunachie, D. Crook, A.J. Pollard, T. Lambe, P. Goulder, N.G. Paterson, M.A. Williams, D.R. Hall, E.E. Fry, J. Huo, J. Mongkolsapaya, J. Ren, D.I. Stuart, G.R. Screaton, Antibody escape of SARS-CoV-2 Omicron BA.4 and BA.5 from vaccine and BA.1 serum, Cell 185 (2022) 2422–2433.e13, https://doi.org/10.1016/j.cell.2022.06.005.
[28] T. Tamura, T. Irie, S. Deguchi, H. Yajima, M. Tsuda, H. Nasser, K. Mizuma, A. Plianchaisuk, S. Suzuki, K. Uriu, M.M. Begum, R. Shimizu, M. Jonathan, R. Suzuki, T. Kondo, H. Ito, A. Kamiyama, K. Yoshimatsu, M. Shofa, R. Hashimoto, Y. Anraku, K.T. Kimura, S. Kita, J. Sasaki, K. Sasaki-Tabata, K. Maenaka, N. Nao, L. Wang, Y. Oda, T. Ikeda, A. Saito, K. Matsuno, J. Ito, S. Tanaka, K. Sato, T. Hashiguchi, K. Takayama, T. Fukuhara, in: Virological Characteristics of the SARS-CoV-2 XBB.1.5 Variant, 2023, https://doi.org/10.1101/2023.08.16.553332. PPR:PPR705749.
[29] M. Salazar-García, S. Acosta-Contreras, G. Rodríguez-Martínez, A. Cruz-Rangel, A. Flores-Alanis, G. Patiño-López, V.M. Luna-Pineda, Pseudotyped vesicular stomatitis virus-severe acute respiratory syndrome-coronavirus-2 S for the study of variants, vaccines, and therapeutics against coronavirus disease 2019, Front. Microbiol. 12 (2022) 817200, https://doi.org/10.3389/fmicb.2021.817200.
[30] M. Chen, X.E. Zhang, Construction and applications of SARS-CoV-2 pseudoviruses: a mini review, Int. J. Biol. Sci. 17 (2021) 1574–1580, https://doi.org/10.7150/ijbs.59184.
[31] J. Moon, Y. Jung, S. Moon, J. Hwang, S. Kim, M.S. Kim, J.H. Yoon, K. Kim, Y. Park, J.Y. Cho, D.H. Kweon, Production and characterization of LV vector-based SARS-CoV-2 pseudoviruses with dual reporters: evaluation of anti-SARS-CoV-2 viral effect of Korean Red Ginseng, J. Ginseng Res. 47 (2023) 123–132, https://doi.org/10.1016/j.jgr.2022.07.003.
[32] S. Pandya, K. Boris-Lawrie, N.J. Leung, R. Akkina, V. Planelles, Development of an Rev-independent, minimal simian immunodeficiency virus-derived vector system, Hum. Gene Ther. 12 (2001) 847–857, https://doi.org/10.1089/104303401750148847.
[33] C. Wu, Q. Xu, H. Wang, B. Tu, J. Zeng, P. Zhao, M. Shi, H. Qiu, Y. Huang, Neutralization of SARS-CoV-2 pseudovirus using ACE2-engineered extracellular vesicles, Acta Pharm. Sin. B 12 (2022) 1523–1533, https://doi.org/10.1016/j.apsb.2021.09.004.
[34] T. Giroglou, J. Cinatl Jr., H. Rabenau, C. Drosten, H. Schwalbe, H.W. Doerr, D. von Laer, Retroviral vectors pseudotyped with severe acute respiratory syndrome coronavirus S protein, J. Virol. 78 (2004) 9007–9015, https://doi.org/10.1128/JVI.78.17.9007-9015.2004.
[35] S. Wang, L. Liu, C. Wang, Z. Wang, X. Duan, G. Chen, H. Zhou, H. Shao, Establishment of a pseudovirus neutralization assay based on SARS-CoV-2 S protein incorporated into lentiviral particles, Biosaf. Health 4 (2022) 38–44, https://doi.org/10.1016/j.bsheal.2021.12.006.
[36] M. Dogan, L. Kozhaya, L. Placek, C. Gunter, M. Yigit, R. Hardy, M. Plassmeyer, P. Coatney, K. Lillard, Z. Bukhari, M. Kleinberg, C. Hayes, M. Arditi, E. Klapper, N. Merin, B.T. Liang, R. Gupta, O. Alpan, D. Unutmaz, SARS-CoV-2 specific antibody and neutralization assays reveal the wide range of the humoral immune response to virus, Commun. Biol. 4 (2021) 129, https://doi.org/10.1038/s42003-021-01649-6.
[37] M.W. Howard, E.A. Travanty, S.A. Jeffers, M.K. Smith, S.T. Wennier, L.B. Thackray, K.V. Holmes, Aromatic amino acids in the juxtamembrane domain of severe acute respiratory syndrome coronavirus S glycoprotein are important for receptor-dependent virus entry and cell-cell fusion, J. Virol. 82 (2008) 2883–2894, https://doi.org/10.1128/JVI.01805-07.
[38] K Dhama, M Dhawan, R Tiwari, et al., COVID-19 intranasal vaccines: current progress, advantages, prospects, and challenges, Hum Vaccin Immunother 18 (2022) 2045853, https://doi.org/10.1080/21645515.2022.2045853.
[39] F. Scialo, A. Daniele, F. Amato, L. Pastore, M.G. Matera, M. Cazzola, G. Castaldo, A. Bianco, ACE2: the major cell entry receptor for SARS-CoV-2, Lung 198 (2020) 867–877, https://doi.org/10.1007/s00408-020-00408-4.
[40] C.B. Jackson, M. Farzan, B. Chen, H. Choe, Mechanisms of SARS-CoV-2 entry into cells, Nat. Rev. Mol. Cell Biol. 23 (2022) 3–20, https://doi.org/10.1038/s41580-021-00418-x.
[41] A. Escalera, A.S. Gonzalez-Reiche, S. Aslam, I. Mena, M. Laporte, R.L. Pearl, A. Fossati, R. Rathnasinghe, H. Alshammary, A. van de Guchte, K. Farrugia, Y. Qin, M. Bouhaddou, T. Kehrer, L. Zuliani-Alvarez, D.A. Meekins, V. Balaraman, C. McDowell, J.A. Richt, G. Bajic, T. Aydillo, Mutations in SARS-CoV-2 variants of concern link to increased S cleavage and virus transmission, Cell Host Microbe 30 (2022) 373–387.e7, https://doi.org/10.1016/j.chom.2022.01.006.
[42] X. Ou, Y. Liu, X. Lei, P. Li, D. Mi, L. Ren, L. Guo, R. Guo, T. Chen, J. Hu, Z. Xiang, Z. Mu, X. Chen, J. Chen, K. Hu, Q. Jin, J. Wang, Z. Qian, Characterization of S glycoprotein of SARS-CoV-2 on virus entry and its immune cross-reactivity with SARS-CoV, Nat. Commun. 11 (2020) 1620, https://doi.org/10.1038/s41467-020-15562-9.
[43] M Laporte, V Raeymaekers, R Van Berwaer, et al., The SARS-CoV-2 and other human coronavirus spike proteins are fine-tuned towards temperature and proteases of the human airways,, PLoS Pathog. 17 (2021) e1009500, https://doi.org/10.1371/journal.ppat.1009500.
[44] M. Lotfi, N. Rezaei, SARS-CoV-2: a comprehensive review from pathogenicity of the virus to clinical consequences, J. Med. Virol. 92 (2020) 1864–1874, https://doi.org/10.1002/jmv.26123.
[45] P. Saha, A.K. Banerjee, P.P. Tripathi, A.K. Srivastava, U. Ray, A virus that has gone viral: amino acid mutation in S protein of Indian isolate of Coronavirus COVID-19 might impact receptor binding, and thus, infectivity, Biosci. Rep. 40 (2020) BSR20201312, https://doi.org/10.1042/BSR20201312.